THE DESIGN OF ULTRA-HIGH QUALITY FEEDBACK AMPLIFIERS

submitted to the

Honors Committee

of the School of Engineering

Tulane University

New Orleans, Louisiana

by Robert E. Rouquette

April 10, 1974

Approved:

Prof. James A. Cronvich

Prof. Paul F. Duvoisin

CONTENTS

ABSTRACT

This paper presents the author's suggestions for reducing high frequency non-linear distortion below the levels achieved in present commercial audio power amplifiers. The commercial amplifiers fail to maintain sufficient negative feedback at the higher working frequencies. Transfer functions are proposed which maintain high negative feedback over the entire range of working frequencies, thus keeping distortion products below a desired design level. The performance of a prototype amplifier using the proposed transfer functions is documented and compared with high quality commercial units. The high frequency non-linear distortion of the prototype amplifier is less than that of the best commercial amplifiers.

In the circuits presented in this paper, an attempt has been made to utilize present silicon transistors to their best advantage. Current mode operation, that is current sources driving low impedances, is used wherever possible. This technique results in good high frequency response, low non-linear distortion, and good thermal stability. The circuits presented, when made to realize the transfer functions proposed, result in an ultra-high quality amplifier.

PART I

TRANSFER FUNCTIONS FOR ULTRA-HIGH QUALITY FEEDBACK AMPLIFIERS

I. Introduction

Presented in this paper are suggestions for improving the quality of commercially available audio-power amplifiers. The present high quality commercial amplifiers all exhibit relatively greater non-linear distortion at the high working frequencies than at the low frequencies. This distortion is audible to a trained ear. The problem is caused mainly by decreasing negative feedback at the high frequencies.

After an examination of basic feedback system concepts, the system used in present commercial practice is analyzed. Next, the relationship between distortion measurements and the results of the analysis will be presented. At this point a system is proposed which will maintain a large amount of negative feedback over the entire range of working frequencies. Lastly, the test results from an amplifier built from the improved system concept are given. The results illustrate that low distortion is maintained in the prototype amplifier over the full working frequency range.

II. Feedback System Concepts

To design an amplifier with a well defined behavior, it is necessary to examine some of the basic concepts of feedback systems. Consider the general system in Fig. 1.

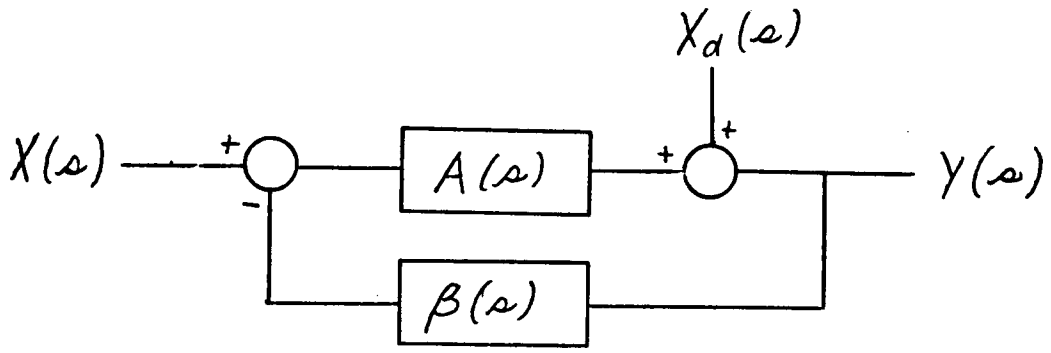

Fig. 1. The general feedback system.

X(s) is the Laplace transform of the signal to be amplified.

$X_d(s)$ is the equivalent signal of the noise and distortion generated within the amplifier referred to the output. This is a useful representation because most of the non-linear distortion is generated in the output stage of a practical amplifier. The transfer functions of the closed loop system are

$$H(s) = \frac{Y(s)}{X(s)} = \frac{A(s)}{1 + A(s)\beta(s)}$$

$$H_d(s) = \frac{Y(s)}{X_d(s)} = \frac{1}{1 + A(s)\beta(s)}$$

Without feedback the distortion and noise signal $X_d(s)$ appears at the output of the system. The relative proportion of $X_d(s)$ to X(s) A(s), which is the desired output, increases with the output signal level for the types of nonlinearities found in actual amplifiers. With the addition of negative feedback, the signal $X_d(s)$ is attenuated by the factor $1 + A(s)\beta(s)$, at the output for the same output signal level. The gain of the system is also reduced by the factor $1 + A(s)\beta(s)$. The quantity $1 + A(s)\beta(s)$ is called the

return difference. The necessary and sufficient criterion for an ultra-high quality feedback amplifier is that the return difference have a large constant magnitude over the working frequency range of the amplifier. This will enable the designer to reduce noise and distortion products to a desired minimum level. [4,5]

III. The Dominant Pole System

As simple as this result is, it is not often followed in common engineering practice. The following example will illustrate this. Figure 2 illustrates the Bode magnitude plot of the transfer function A(s) for a large group of amplifiers. To ensure closed loop stability, a single pole at ω_2 is made to dominate the high frequency response by one of the many techniques available. The remaining poles are constrained to lie at frequencies above

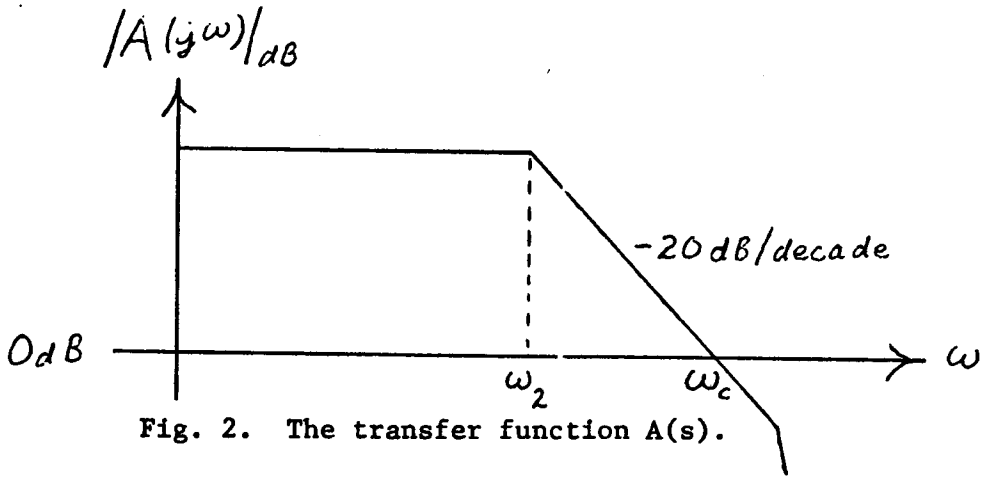

Fig. 2. The transfer function A(s).

the magnitude crossover; i.e., at frequencies above ω_c. To accomplish this with a minimum of amplifier stages requires that ω_2 be well within the range of operating frequencies. For an audio amplifier, which operates from 20 Hz to 20 kHz, $f_2 = \omega_2/2\pi$ is often near 1 kHz.

Let us now look at the closed loop system with

$$A(s) = \frac{K}{1 + s/\omega_2}$$

This is a good practical choice of transfer function because it yields simple analytical results which are easy to interpret, and it is a good representation of the forward gain of many commercial amplifiers with the stability compensating elements included. The system is redrawn in Fig. 3 with the Bode magnitude plot of the important transfer functions. F(s) is the inverse of the return difference. It is evident that the return difference $1 + A(s)\beta(s) = 1/F(s)$ decreases in magnitude above ω_2 at 20 dB/decade until it reaches 0 dB. Thus the benefits gained from negative feedback, which are directly proportional to the return difference, decrease above ω_2. It should be noted that ω_2 is often within the working frequency range of commercial amplifiers. The constant value of $\beta = 1/B$ assumed here is reasonable since the β network in usually a resistive divider. The closed loop transfer function can be approximated by

$$H(s) = \frac{B}{1 + s/\frac{K}{B}\omega_2} \quad \text{for } \frac{K}{B} \gg 1$$

The wide bandwidth of commercial amplifiers is accounted for by the K/B coefficient of ω_2.

IV. The Relation of Harmonic and Intermodulation Distortion Measurements to Return Difference

As shown in Section II on feedback system concepts, the distortion products $X_d(s)$ are attenuated by the return difference $1 + A(s)\beta(s)$. $X_d(s)$ is

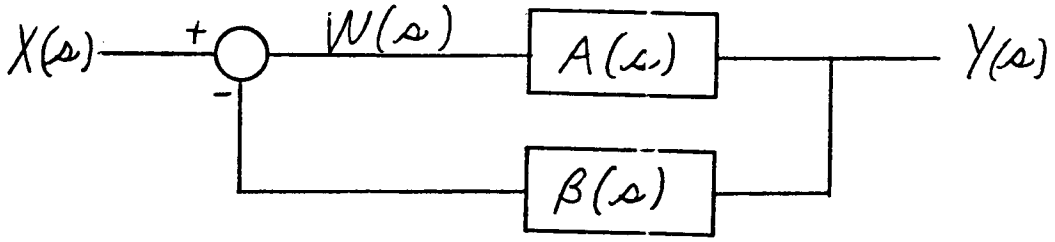

$$A(s) = \frac{K}{1 + s/\omega_2} \qquad B(s) = \frac{1}{B}$$

$$H(s) = \frac{Y(s)}{X(s)} = \frac{A(s)}{1 + A(s)B(s)} = \frac{K}{(1 + K/B)} \frac{1}{(1 + s/(1 + \frac{K}{B})\omega_2)}$$

$$F(s) = \frac{W(s)}{X(s)} = \frac{1}{1 + A(s)B(s)} = \frac{1}{(1 + K/B)} \frac{(1 + s/\omega_2)}{(1 + s/(1 + \frac{K}{B})\omega_2)}$$

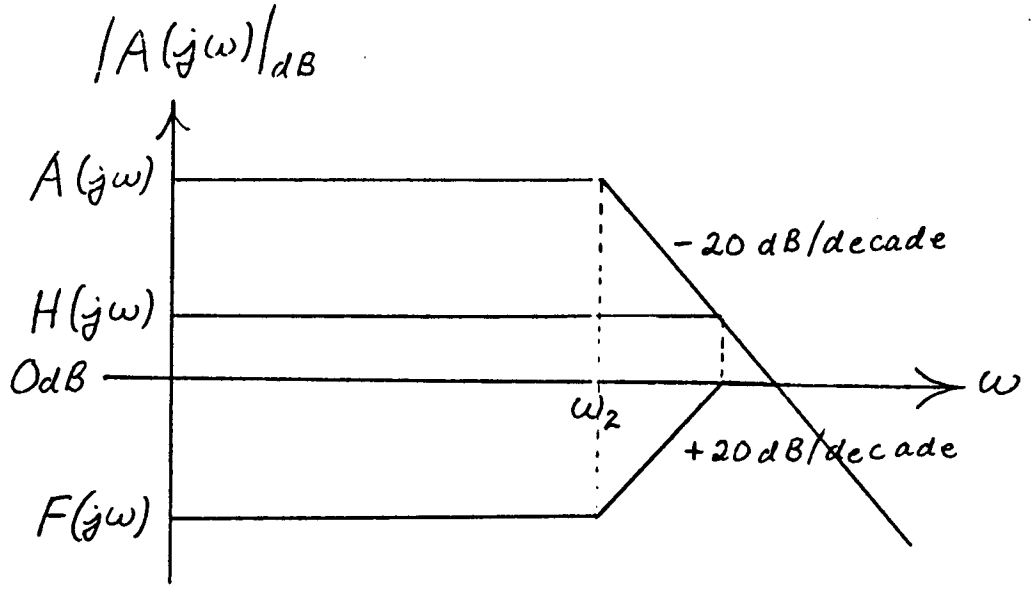

Fig. 3. The dominant pole system.

the signal composed of the noise and the non-linear distortion products generated in the output stage. A quantitative analysis of the components of $X_d(s)$ may be had by representing the static non-linearities of the amplifier by a Taylor series of the form

$$y(t) = Ax(t) + Bx^2(t) + Cx^3(t)$$

The third order approximation is usually of sufficient accuracy to describe real amplifiers.

Sinusoidal waveforms are convenient for testing amplifiers. If the input $x(t) = V_1 \cos \omega_a t + V_2 \cos \omega_b t$ is used, the output y(t) will contain the amplified input signal plus the distortion products shown in Table 1. $X_d(s)$ is the Laplace transform of the distortion products given in Table 1. For the electronic components used in amplifiers the coefficients A,B, and C in the Taylor series may be considered constants with negligible error over the range of audio frequencies. Thus for a given signal level the magnitude of the distortion signal generated is independent of frequency. For a given signal level variations in magnitude of the return difference with frequency will cause variations in magnitude of the distortion products at the output since they are attenuated by the return difference.

In the dominant pole system of Section III, the return difference decreases above ω_2. Due to the decreasing return difference above ω_2 the percent harmonic and intermodulation distortion measured for this system should increase above ω_2. This is the case in commercial amplifiers in most of which ω_2 is in the working range of frequencies. Harmonic distortion data for two representative commercial amplifiers is listed in Table 2. An amplifier

designed with a constant return difference over the working frequency range should exhibit uniformly low distortion products. This would be an improvement over present commercial practice.

$$y(t) = \tfrac{1}{2} B (V_1^2 + V_2^2)$$
$$(A V_1 + \tfrac{3}{4} C V_1^3 + \tfrac{3}{2} C V_1 V_2^2) \cos \omega_a t$$
$$(A V_2 + \tfrac{3}{4} C V_2^3 + \tfrac{3}{2} C V_1^2 V_2) \cos \omega_b t$$
$$\tfrac{1}{2} B V_1^2 \cos 2\omega_a t$$
$$\tfrac{1}{2} B V_2^2 \cos 2\omega_b t$$
$$\tfrac{1}{4} C V_1^3 \cos 3\omega_a t$$
$$\tfrac{1}{4} C V_2^3 \cos 3\omega_b t$$
$$B V_1 V_2 (\cos(\omega_a + \omega_b)t + \cos(\omega_a - \omega_b)t)$$
$$\tfrac{3}{4} C V_1^2 V_2 (\cos(2\omega_a + \omega_b)t + \cos(2\omega_a - \omega_b)t)$$
$$\tfrac{3}{4} C V_1 V_2^2 (\cos(\omega_a + 2\omega_b)t + \cos(\omega_a - 2\omega_b)t)$$

Table 1. The components of y(t) for $x(t) = V_1 \cos \omega_a t + V_2 \cos \omega_b t$.

FREQUENCY	20	200	2k	20k	Hz	
% TOTAL HARMONIC DISTORTION	.001	.002	.02	0.2	CROWN DC-300 150 WATTS RMS INTO 8 OHMS	
	0.3	0.1	0.1	1.0	AUDIO RESEARCH DUAL 75A 75 WATTS RMS INTO 8 OHMS	

Table 2. Harmonic distortion data for two commercial amplifiers. [6,7]

V. The Constant Return Difference System

A different approach to the design of the feedback amplifier, developed by the author, will now be presented. It will result in a large return difference that is constant with frequency over the working frequency range of the amplifier. Consider the system building block in Fig. 4. Note that $\beta(s)$ is altered. Some points must be made regarding this system. The break frequency ω_2 must be comfortably above the working frequency range of the system. For audio work with an upper band limit of 20 kHz, 80 kHz was chosen for f_2. Not obvious, perhaps, is the result that the closed loop frequency response is determined by the zero in the β network. Actually the closed loop response can be approximated by

$$H(s) = \frac{1}{\beta(s)} = \frac{B}{1 + s/\omega_2} \quad \text{for} \quad \frac{K}{B} \gg 1$$

To build a practical amplifier with a constant return difference over the working range of frequencies some further development of the technique is required.

VI. The Cascade of Constant Return Difference Blocks

The constant return difference is gained at some expense. In an actual amplifier there are additional poles above ω_2 in the forward response. The additional phase shift contributed by these poles will cause the amplifier to be unstable when the feedback loop is closed unless relatively small values of K are used. To obtain a large return difference K must be large so several of these building blocks must be cascaded. The format is shown in Fig. 5.

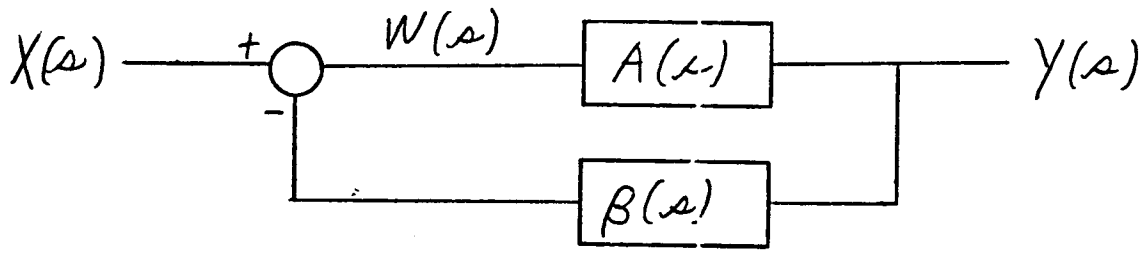

$$A(s) = \frac{K}{1 + s/\omega_2} \qquad \beta(s) = \frac{1}{B}(1 + s/\omega_2)$$

$$H(s) = \frac{Y(s)}{X(s)} = \frac{A(s)}{1 + A(s)\beta(s)} = \frac{K}{(1 + K/B)(1 + s/\omega_2)}$$

$$F(s) = \frac{W(s)}{X(s)} = \frac{1}{1 + A(s)\beta(s)} = \frac{1}{1 + K/B}$$

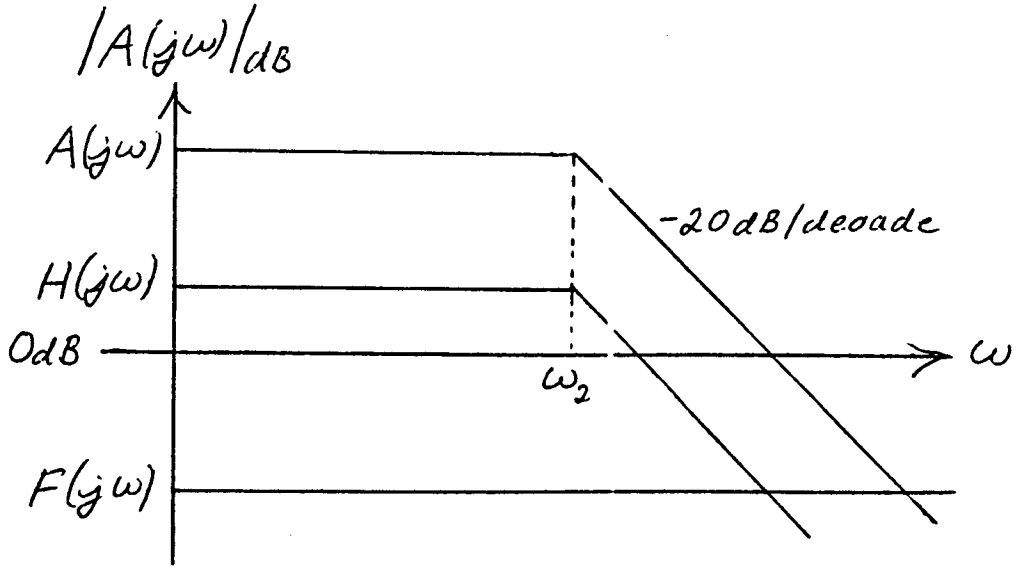

Fig. 4. The constant return difference system.

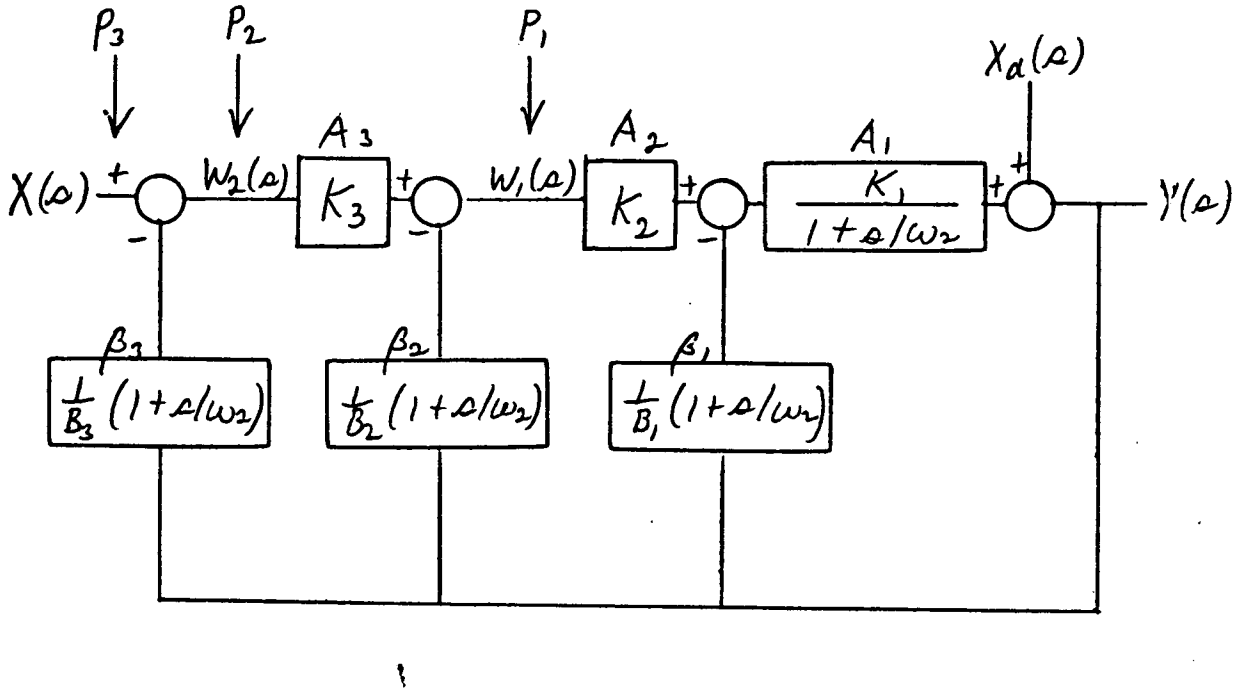

Fig. 5. The constant return difference cascade.

The transfer function from each point P_i to the output is of the form

$$\frac{Y(s)}{W_i(s)} = \frac{K_{i+1}\, B_i}{1 + s/\omega_2}$$

before the loop to the left of it is closed. Thus the analysis in Part V holds for each loop that is closed proceeding to the left. The overall return difference may be obtained as follows. A distortion signal $X_d(s)$ is introduced at the output as is the basic feedback system. To solve for the system transfer functions we obtain

$$Y = A_1A_2A_3X + X_d - A_1A_2A_2\beta_3Y - A_2A_3\beta_2Y - A_3\beta_1Y$$

The argument (s) has been omitted for simplicity. After some algebraic manipulation the resulting transfer functions are found to be

$$H(s) = \frac{Y(s)}{X(s)} = \frac{A_1 A_2 A_3}{1 + A_1 A_2 A_3 \beta_3 + A_1 A_2 \beta_2 + A_1 \beta_1}$$

$$H_d(s) = \frac{Y(s)}{X_d(s)} = \frac{1}{1 + A_1 A_2 A_3 \beta_3 + A_1 A_2 \beta_2 + A_1 \beta_1}$$

The overall return difference is the denominator of the two equations above. Usually $K_{i+1} B_i / B_{i+1} \gg 1$ in which case the return difference may be approximated by $K_1 K_2 K_3 / B_3$.

The reader may note the same approximate return difference would be obtained without the two inner feedback loops. The two inner loops are needed in a real amplifier to achieve closed loop stability. In the actual amplifier there are additional poles in the forward gain blocks above ω_2. If we consider the basic feedback system of Fig. 4 with the new forward gain

$$A(s) = \frac{K}{(1 + s/\omega_2)(1 + s/\omega_H)}$$

$$\beta(s) = \frac{1}{B}(1 + s/\omega_2)$$

Then

$$H(s) = \frac{K}{(1 + \frac{K}{B})} \frac{1}{(1 + s/\omega_2)} \frac{1}{(1 + s/(1 + \frac{K}{B})\omega_H)}$$

Where $1/(1 + s/\omega_H)$ represents an additional pole in the forward gain of an actual amplifier. On closing the feedback loop the pole at ω_H is moved to the higher frequency $(1 + \frac{K}{B})\omega_H$. Since $K/B \gg 1$ in these designs, the additional poles above ω_2 in each inner loop are moved far enough up in frequency so as

not to affect the closed loop stability of the next outer loop. Without the inner feedback loops the additional poles above ω_2 in the blocks A_1 and A_2 would cause instability when the outer loop is closed. Therefore, with $K_1 = K_2 = 100$, $K_3 = 10{,}000$, $B_1 = B_2 = 1$, and $B_3 = 100$ an overall return difference of 10^6 independent of frequency over the working range can be obtained while maintaining closed loop stability. The resulting amplifier using this feedback configuration should exhibit a constant value of harmonic or intermodulation distortion below the design limit for any frequency(s) in the operating frequency range of the amplifier.

An additional feature of the constant return difference building blocks is concerned with the dynamic range of an actual amplifier. As shown previously, the inverse of the return difference is the transfer function from the input X(s) to the drive signal of the amplifier W(s). In the dominant pole system, which is characteristic of most commercial amplifiers, the magnitude of W(s) (see Fig. 3) is greater at the high frequencies than at the low frequencies. The dynamic range of the input stages is that required to ensure linear signal swings at the high frequencies. To obtain wide dynamic range it is necessary that large values of quiescent current or voltage be used. This requirement is contrary to the one that low quiescent levels be used for a good noise figure in the input stage. With the constant return difference scheme F(s) = W(s)/X(s) (see Fig. 4) is very small and constant with frequency in the operating frequency range. The input stages of this type of amplifier operate with very small signal swings. Adequate dynamic range may be provided with small quiecent levels and a better noise figure results than in the dominant pole system. A time domain analysis of the

response to a step input yields the same constraints for the dynamic range of the input stages as the preceeding frequency domain analysis for the two systems. [1,2]

VII. The Prototype Amplifier

A prototype amplifier has been built using constant return difference techniques. The block diagram of the amplifier is shown in Fig. 6.

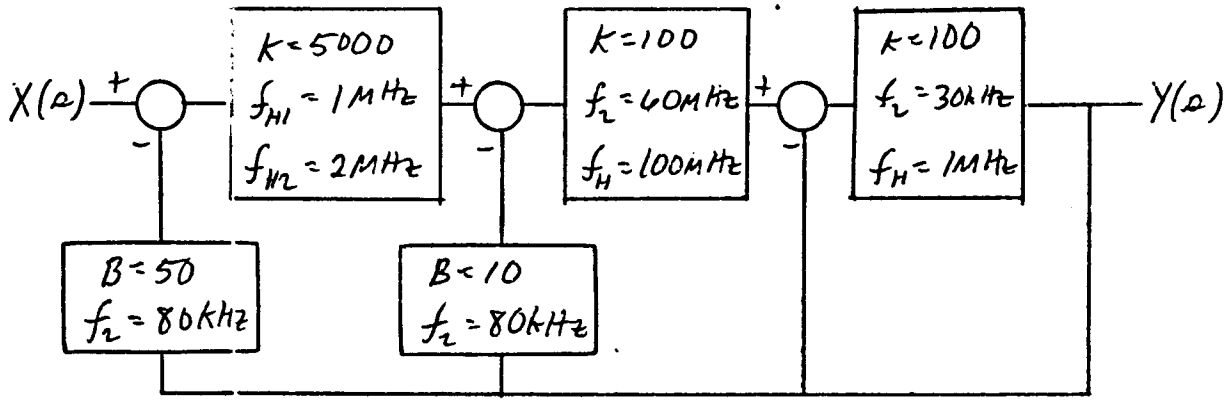

Fig 6. Block diagram of the prototype amplifier.

The values of K and the break frequencies $f_2 = \omega_2/2\pi$ corresponding to the transfer functions in Fig. 5 are shown. The reader will note a variation in the output stage in that unity feedback is used. This is due to the emitter follower output stage. Nevertheless, this is a constant return difference scheme. A partial schematic diagram of the amplifier is given in Fig. 7. The power supply and dissipation limiting circuitry for the output transistors have been omitted for clarity.

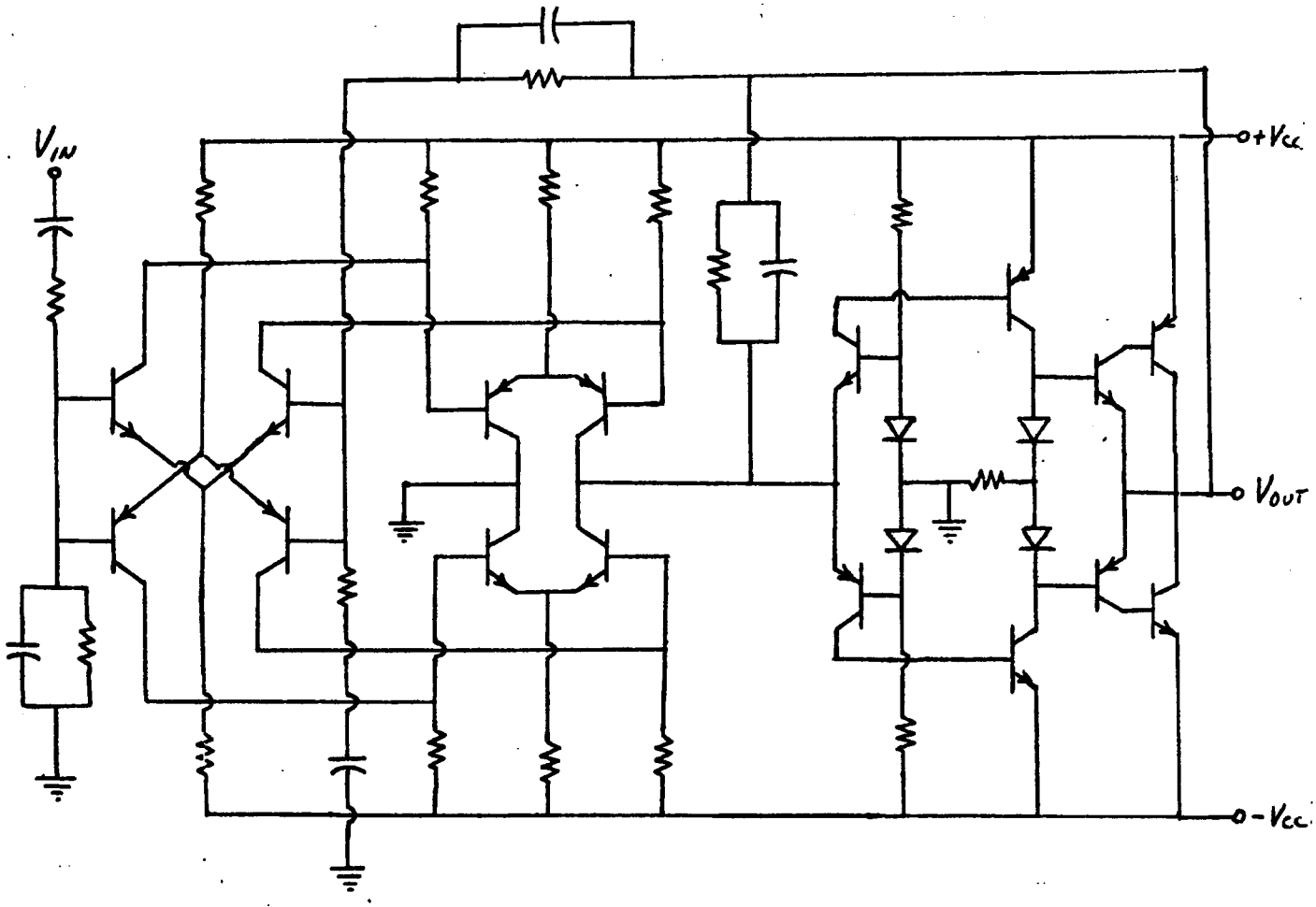

Fig. 7. Schematic diagram of the prototype amplifier.

The measured distortion products of the prototype amplifier are listed in Table 3.

The measured values of distortion for the prototype amplifier verify that low values of distortion over the entire working frequency range may be obtained using constant return difference techniques.

FREQUENCY	20	200	2K	20K	Hz
% TOTAL HARMONIC DISTORTION	.04	.04	.04	.04	PROTOTYPE AMPLIFIER 20 WATTS RMS INTO 8 OHMS

% TOTAL INTERMODULATION DISTORTION	0.10	FOR 500 Hz AND 10 kHz MIXED		1:1
	0.04	500 Hz	400 Hz	1:1
	0.16	10 kHz	10.5 kHz	1:1

THE PEAK POWER IN THE INTERMODULATION TEST IS THE SAME AS THAT IN THE HARMONIC DISTORTION TEST. THE LOAD IMPEDANCE IS 8 OHMS.

Table 3. Measured distortion products of the prototype amplifier.

VIII. Conclusion

The shortcomings of present commercial amplifier design in the area of high frequency non-linear distortion have been exposed. A theoretical analysis of the dominant pole feedback system, which comprises these amplifiers, has been presented. The constant return difference feedback technique was developed which results in uniform distortion reduction over the entire working range of frequencies. Lastly, a prototype amplifier was built. Distortion measurements of this amplifier verified the constant return difference analysis.

The author feels that the information in this paper demonstrates the need for more complete documentation of amplifier performance by manufacturers. Specifically, a graph of total harmonic distortion vs. frequency from 20 Hz to 20 kH_z at full power output should be provided. Crown and Audio Research are two of the manufacturers who do this. Many manufacturers simply publish the total harmonic distortion at full power output at the mid-frequencies. Intermodulation tests are more stringent than harmonic distortion tests. In addition to the standard intermodulation test using 60 and 7000 Hz mixed 4:1, a high frequency intermodulation test, say 10 and 11 kH_z mixed 1:1 would be very revealing of amplifier quality. These tests should be made at power levels from milliwatts to full power output, and graphs of total intermodulation distortion vs. power output published. The more reputable manufacturers already provide most of this data. The table of data for the prototype amplifier lists some of these measurements. This concludes the author's recommendations for amplifier testing.

PART II

CIRCUIT DESIGNS FOR ULTRA-HIGH QUALITY FEEDBACK AMPLIFIERS

I. Introduction

An ultra-high quality amplifier must surpass high quality commercial amplifiers in performance. The improved distortion characteristics of the prototype amplifier were discussed in Part I. The circuits described in this section were designed to equal or surpass present commercial practice in the following areas: 1. non-linear distortion reduction, 2. noise reduction, 3. power conversion efficiency, 4. power supply ripple rejection, 5. thermal stability, and 6. economy of design. General design considerations in the above areas are presented first. A detailed treatment of the output, driver, and input stages follows. Experimental results are then presented which document the superior performance of the prototype amplifier.

II. Economics

Before discussing the actual circuitry, it will be expedient to look at some general design concepts which have been adopted during the project. The goal was to design an economical audio power amplifier with lower distortion products

than is presently available commercially. This can best be achieved by using silicon technology. The output transistors Q1 and Q2 cost $2.55 for the pair. The remaining transistors used in the amplifier cost 56¢ each. 5% tolerance carbon composition resistors are used exclusively. Capacitors of small value are polystyrene, and the two electrolytics are tantalum. The capacitors must be of this high quality to ensure realization of the benefits of the circuit design. A simple capacitor filter power supply is required. The components listed above are equivalent to those found in present commercial units of high quality. The manufacturing steps are similar, and the labor required is the same. High reliability and repeatability are easily obtained. Therefore, this design is economically competitive with present comercial designs.

III. Non-linear Distortion Reduction

It is desirable to reduce the inherent non-linear distortion of each amplifier stage before the application of negative feedback. The first step in the design is the use of the push-pull configuration for the entire amplifier. This is feasible and desirable because of the availability of inexpensive high quality complementary silicon transistors. The entire amplifier is a complementary-symmetry design. The pullout on page 34 is the complete schematic of the amplifier (Fig.13). The push-pull configuration results in non-linear distortion reduction of about 5 to 1 for the large signal

driver and output stages. Another advantage of the completely push-pull design is that active drive is present on both positive and negative signal swings. There are no passive collector load impedances. This improves the high frequency response of the various stages and makes feedback stability compensation easier. Active drive also speeds up recovery time if the amplifier is driven into saturation. Other benefits are probably present of which the author is not yet fully aware.

The next step in non-linear distortion reduction is to eliminate the input junction non-linear voltage-current characteristic. This is easily accomplished by driving each input junction from a current source such as the collector of the preceding stage. This configuration is used throughout the amplifier. Under certain conditions this is not possible due mainly to thermal stability considerations. In these cases a silicon diode is placed in parallel with the input junction, and the parallel combination is driven by a current source. The current flowing into the parallel combination will divide proportionally between the two junctions over a wide range of current levels because the two voltage-current characteristics track each other. The ratio of the current division is determined by doping levels, device geometry, and operating point. Nevertheless, this configuration minimizes the effect of input junction non-linearity as opposed to driving the junction from a voltage source.

The remaining significant distortion mechanism is the β non-linearity of the transistors. The β of the output transistors Q1 and Q2 decreases by more than 4 to 1 as the 2.25 ampere peak output current is approached. The β variation of the remaining transistors is not more than 2 to 1. The current gain vs. collector current is included in the device data sheets in the appendix. With the circuit designs used to minimize input junction non-linearities, the β non-linearities become the dominant distortion mechanism in the amplifier. The other non-linear effects associated with the transistors, such as junction capacitance variation with voltage, are also less significant than the β variations. The negative feedback is used to reduce the remaining non-linear distortion to an acceptable level. An acceptable level is less than .1% harmonic or intermodulation distortion at any frequency between 20Hz and 20kHz at any power level.

IV. Power Supply Ripple Rejection

High power supply ripple rejection is desirable from an economic viewpoint. With high ripple rejection a simple capacitive filter power supply may be used. This eliminates the need for two expensive high current filter chokes. High ripple rejection also eliminates the need for a regulated power supply to maintain constant quiescent operating points. Another benefit is that signal voltages produced across power supply impedances will not couple back into the amplifier

signal paths. This permits one power supply to be used in a two channel system without adjacent channel crosstalk through the power supply.

The circuit design to achieve high power supply ripple rejection is consistent with that used to minimize non-linear distortion. The requirement is that only current sources transfer signals between circuits referenced to ground and circuits referenced to a power supply potential. Thus, the collector junction current sources, which minimize input junction non-linearities, also provide high power supply ripple rejection and enhance the economy of the design.

V. Thermal Design

The power dissipation of each stage and the heat sinking required will be discussed in later sections. However, a problem of general interest is thermal stability with silicon transistors. Circuit failures during early work on the project indicated that an in depth thermal stability analysis was required. [5] The model used for the analysis is shown in Fig. 8.

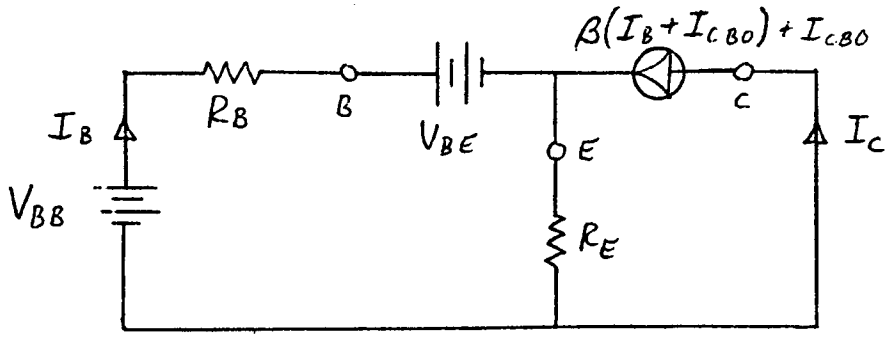

Fig. 8. The model for thermal stability analysis.

This model was chosen so that the effects of I_{CBO}, V_{BE}, and β variations on the collector current could be analyzed. The stability factors calculated from the model are:

$$S_{I_{CBO}} = \frac{\partial I_C}{\partial I_{CBO}} = \frac{(\beta+1)(R_B+R_E)}{R_B+(\beta+1)R_E}$$

$$S_{V_{BE}} = \frac{\partial I_C}{\partial V_{BE}} = \frac{-\beta}{R_B+(\beta+1)R_E}$$

$$S_\beta = \frac{\partial I_C}{\partial \beta} = \frac{(V_{BB}-V_{BE}+R_E I_{CBO})(R_B+R_E)}{(R_B+(\beta+1)R_E)^2}$$

The use of stability factors in thermal design proceeds as follows. An incremental increase in temperature is assumed. The change in collector current due to the change in a given parameter is obtained from the stability factor. The power dissipation from the new collector current is calculated. The temperature change accompanying the new power dissipation is determined. If the temperature change calculated is less than that assumed originally, then thermal runaway cannot occur. This approach forms the basis of the following discussion.

Most conventional transistor amplifier biasing circuits were developed for germanium transistors in which I_{CBO}, the collector-base leakage current, was the dominant cause of thermal runaway. After consulting the data sheets in the appendix, it becomes obvious that for temperatures below 100°C I_{CBO} for the transistors used is negligable. Changes of V_{BE} with temperature form the major contribution to thermal instability with silicon transistors. ΔV_{BE} is approximately 200 mvolts for a ΔT of 100°C. For small R_B and large R_E, which minimizes

$S_{I_{CBO}}$, $S_{V_{BE}}$ becomes large. Since the effect of I_{CBO} is negligable, a current source drive ($R_B \to \infty$) will essentially eliminate collector current variations due to V_{BE} changes. $R_E = 0$ since it has no effect on thermal stability with current source drive. In addition to improving linearity and power supply ripple rejection, current drive also enhances thermal stability.

The differential amplifiers used in the input stage are thermally stable for a different reason. Here R_B is a relatively low resistance and R_E is very large. However, the collector current is held constant within 2% for a ΔT of 100°C. This is so because the voltage drop across the emitter resistor, which is $2I_{CQ}R_E$, is equal to 10 volts + ΔV_{BE}, where ΔV_{BE} is 200 mvolts for $\Delta T = 100°C$.

The circuit configuration of the diode in parallel with the input junction of a transistor is very temperature stable. Besides the tracking of the voltage-current characteristic, the temperature dependence of this characteristic is similar if both junctions are silicon. Furthermore, thermal feedback may be used to improve thermal stability. The diode may be connected to the heat sink of a following stage. If the temperature of the stage rises, the diode current increases for a given V_{BE} so that current is diverted from the transistor input into the biasing diode. This technique is used in the output stage.

In the differential amplifiers changes in β do not appear as changes in the collector current

because the collector current is set by the voltage drop across R_E. (The base bias current changes.) However, in the other two cases driven by current sources, changes in β cause changes in collector current. For the silicon transistors used β varies 2 to 1 for $\Delta T = 100^{\circ}C$. Doubling β would result in doubling the quiescent power dissipation in the circuits used. Doubling the power dissipation produces far less than a change of $100^{\circ}C$ in the junction temperature of the transistor with the cooling provided. Thus, thermal runaway cannot occur. This concludes the discussion of general design features. The actual circuitry of the prototype amplifier will now be described.

VI. The Output Stage

The output stage is shown in Fig. 9.

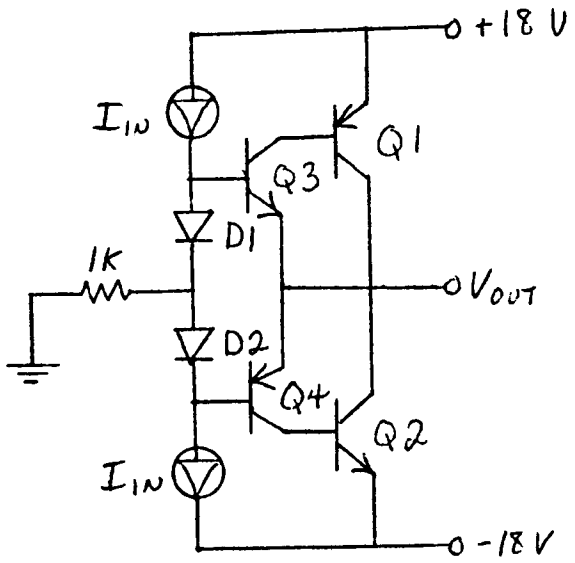

Fig. 9. The output stage.

The current sources represent the output of the driver stage. Current source drive is used for Q1 and Q2 for the reasons previously discussed. Likewise, a current source drives Q3 and Q4 which are shunted by diodes D1 and D2. D1 and D2 are mounted on the output transistor heat sink to increase thermal stability. Unity voltage feedback is applied to the emitters of Q3 and Q4. This is the unity feedback loop in the block diagram of the amplifier in Part I. As indicated in the data sheets, the high frequency rolloff of Q1 and Q2 is 30 kHz and that of Q3 and Q4 is 1 MHz. The 30 kHz break point was verified experimentally. The -3 dB point with the feedback loop closed is 3 MHz indicating a return difference of about 100.

The unity feedback output stage is required as a buffer. The amplifier should exhibit low distortion and closed loop stability for any passive load impedance greater than or equal to 8 ohms. It is therefore necessary that the voltage gain and frequency response of the output stage not vary with load impedance. With an 8 ohm load the input impedance at the bases of Q3 and Q4 is about 10 kohms. This input impedance is shunted by the 1 kohm load resistor for the driver stage. Thus, the driver sees a fairly constant resistive load impedance rgardless of the load on the amplifier. This, along with the unity feedback, does indeed keep the voltage gain and frequency response of the output and driver stages essentially constant with varying load.

The output and driver stages are operated class AB as a compromise between high power conversion efficiency and

low non-linear distortion. The quiescent collector current of the output transistors Q1 and Q2 is 300 ma. The full load peak collector current is 2.25 amps. This is a relatively high output quiescent current, but, in conjunction with the input biasing diodes D1 and D2, it completely eliminates crossover distortion.

The heat sink selected for Q1 and Q2 has a thermal resistance of $4^{\circ}C/W$. The transistor must be able to dissipate 10 watts in an ambient temperature of $100^{\circ}C$. From the power derating curve in the data sheets, the case temperature must not exceed $150^{\circ}C$. Therefore, the heat sink thermal resistance must be

$$\theta_{CA} \leq \frac{150^{\circ}C - 100^{\circ}C}{10\ W} = 5^{\circ}C/W$$

Furthermore, when operating with an 8 ohm or greater load impedance, the signal levels lie completely within the safe operating area specified in the data sheets. The remaining transistors in the amplifier do not require external heat sinks and are all operated within their safe limits.

Protection is not provided for loads less than 8 ohms. At this point in the project, work has not been done on output transistor dissipation limiting circuitry. This circuitry is required to protect the output transistors from overheating when low impedance loads or short circuits are applied to the amplifier. Output dissipation limiting circuitry is used in all high quality commercial power amplifiers. The developement of this circuitry is a subject for future work.

VII. The Driver Stage

The driver stage is shown in Fig. 10.

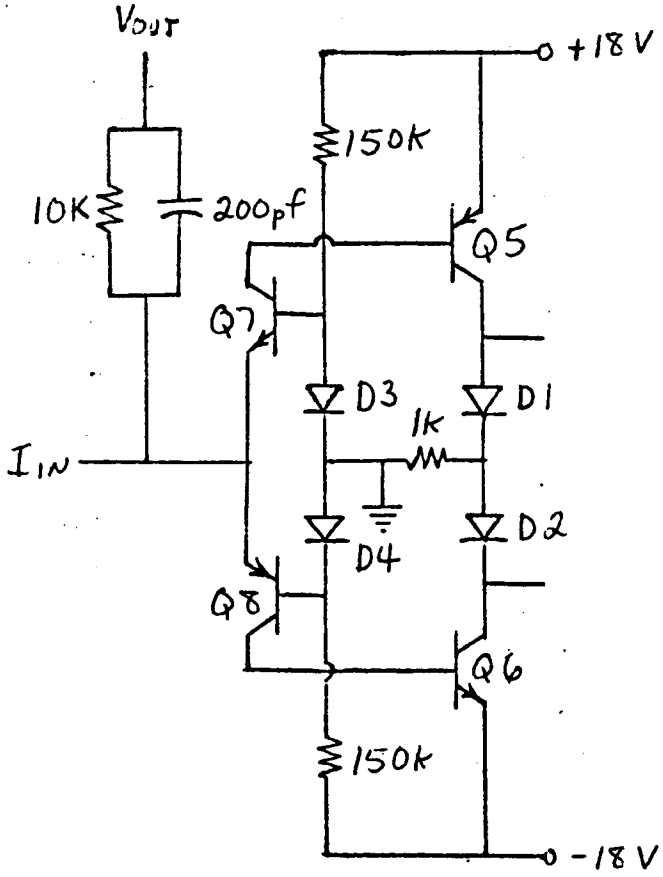

Fig. 10. The driver stage.

The current I_{in} is supplied by the input stage. Current source drive is used for Q5 and Q6 for the reasons presented earlier. Q7 and Q8 are common base amplifiers. This configuration has many advantages. The quiescent operating points of the class AB driver and output stages are set by the current supplied through the 150 kohm resistors. Thus, the input stages supply only signal drive, not bias current. This provides a margin of thermal stabilty not often found in direct coupled

amplifiers. Diodes D3 and D4, in addition to providing the benefits mentioned previously, provide a low impedance point for the bases of the common base amplifiers. The low input impedance of Q7 and Q8 facilitates the application of current shunt feedback from the output of the amplifier.

The high frequency rolloff of Q5 and Q6 with the 1 kohm load resistor is 60 kHz. That of the common base amplifiers is 100 MHz (from the data sheet). This rolloff at 60 kHz is near enough to the desired 80 kHz rolloff called for in Part I. A zero at 80 kHz is provided in the feedback network by the 10 kohm resistor and the 200 pf capacitor. This circuit realizes the driver section of the block diagram of the protoype amplifier in Part I.

The buffering capabilty of the output stage was verified in the lab. With the driver feedback loop open, the high frequency rolloff is at 60 kHz with an 8 ohm resistive load. On removing the load the break frequency moved to 40 kHz and the gain increased by 30%. This change in gain and pole location is well tolerated when the feedback loop is closed. The closed loop response of the driver and ouput stages rolls off at 80 kHz with a negligible shift in pole location and gain from no load to full load. Another advantage of the circuit configuration of the driver and output stages is that the output signal may swing linearly to within 1 volt of the power supply potentials. This enhances the power conversion efficiency of the design.

VIII. The Input Stage

To complete the design the input stage must be added. It is shown in Fig. 11.

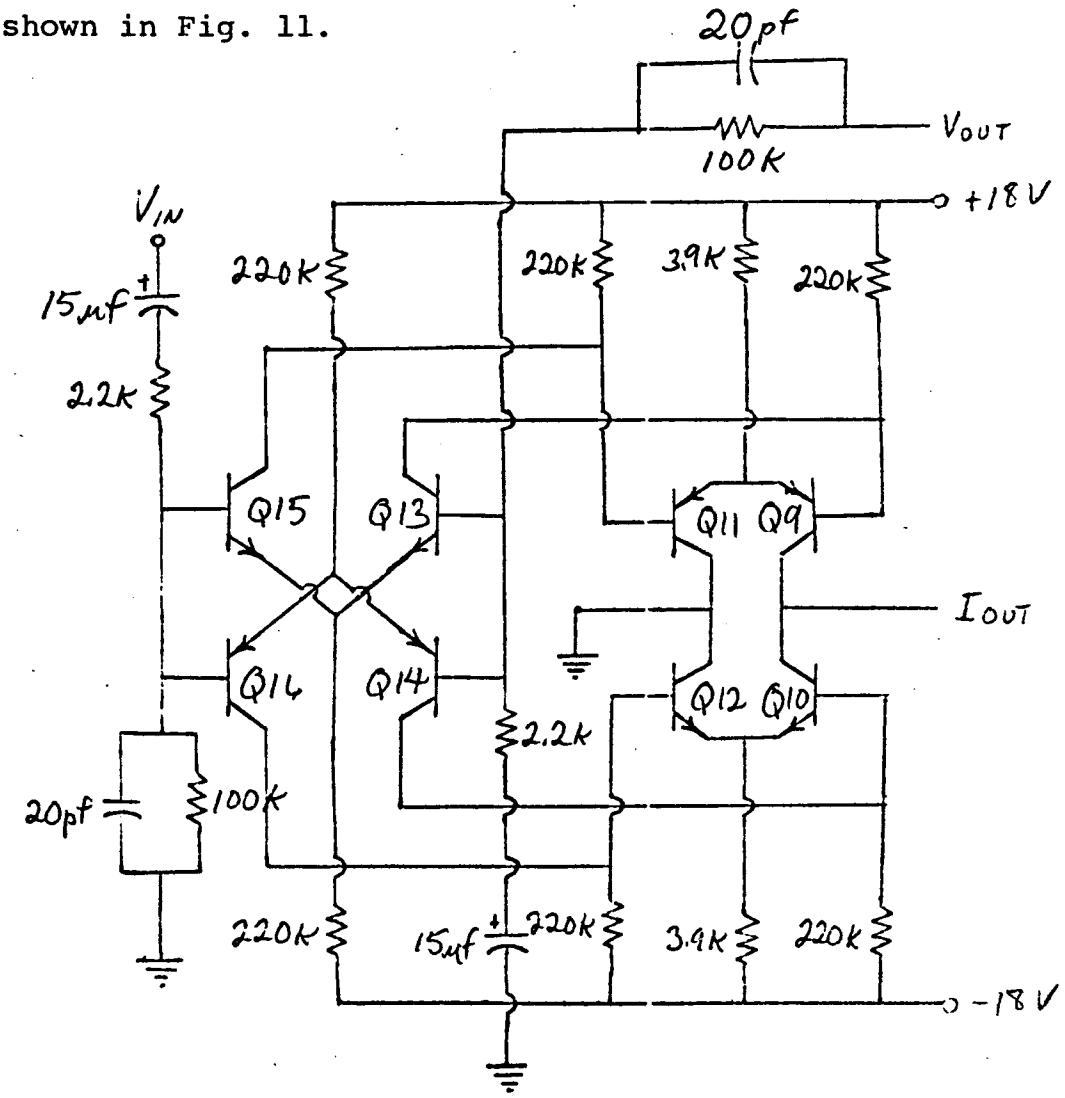

Fig. 11. The input stage.

This stage consists of two push-pull differential amplifiers. Some characterstics previously discussed are the low non-linear distortion, the power supply ripple rejection, and the thermal stability. Internally generated noise presents no problem in the driver and output stages. However, the

input amplifiers operate with high gain and low signal levels. Thus, the noise figure of the input stage should be kept as low as possible. A low noise figure is obtained by operating at low quiescent current levels and with low source impedances. The quiescent collector current of Q13, Q14, Q15, and Q16 is 40μa. The source resistance is 2.2 kohms. This operating point results in a noise figure of about 4 dB from the data sheets. Linearity is maintained with this low quiescent current over the entire operating range of frequencies as a direct consequence of the constant return difference feedback scheme. (See page 12.) The noise figure of Q9, Q10, Q11, and Q12 is comparably low. The adequacy of these noise figures is verified in that the signal to noise ratio of the amplifier referenced to full power output is greater than 90 dB.

The input stage is operated class A for good linearity. The quiescent collector current in each transistor is indicated below it in the complete schematic diagram in Fig. 13. Also given are the collector currents at peak signal swing with an 8 ohm resistive load. The high frequency rolloff of the input transistors Q13, Q14, Q15, and Q16 is about 1 MHz. That of Q9, Q10, Q11, and Q12 is about 2 MHz. A zero at 80 kHz is provided in the feedback path from the output by the 100 kohm resistor and tne 20 pf capacitor. This circuit realizes the input block in Fig. 6 of Part I. This input stage completes the physical realization of the constant return difference feedback system proposed in Part I. In addition to the single

pole high frequency rolloff at 80 kHz, which characterizes the closed loop high frequency response, the two 15μf capacitors in the input circuitry produce a single pole low frequency rolloff at 5 Hz in the closed loop response. This concludes the circuit description of the prototype amplifier.

IX. Measured Performance

The results of distortion measurements have been presented in Part I. A comparison of the harmonic distortion data of the prototype amplifier and two high quality commercial units is repeated in Fig. 12. The input impedance of the amplifier was found to be 100 kohms resistive from 20 Hz to 20 kHz. The output impedance is 0.06 ohm resistive from 20 Hz to 20 kHz. A constant low output impedance over the entire range of operating frequencies is not achieved in present commercial practice. Since the output impedance is also determined by the return difference, the benefits discussed in Part I in terms of distortion reduction also apply to the output impedance. The midband voltage gain of the amplifier is 45 with the -3 dB points at 5 Hz and 80 kHz. The asymptotic rolloff is 6 dB per octave. Thus, the response is 0.5 dB down at 20 Hz and 20 kHz. This is a desirable frequency response for an audio power amplifier. The signal to noise ratio referenced to full power output is greater than 90 dB.

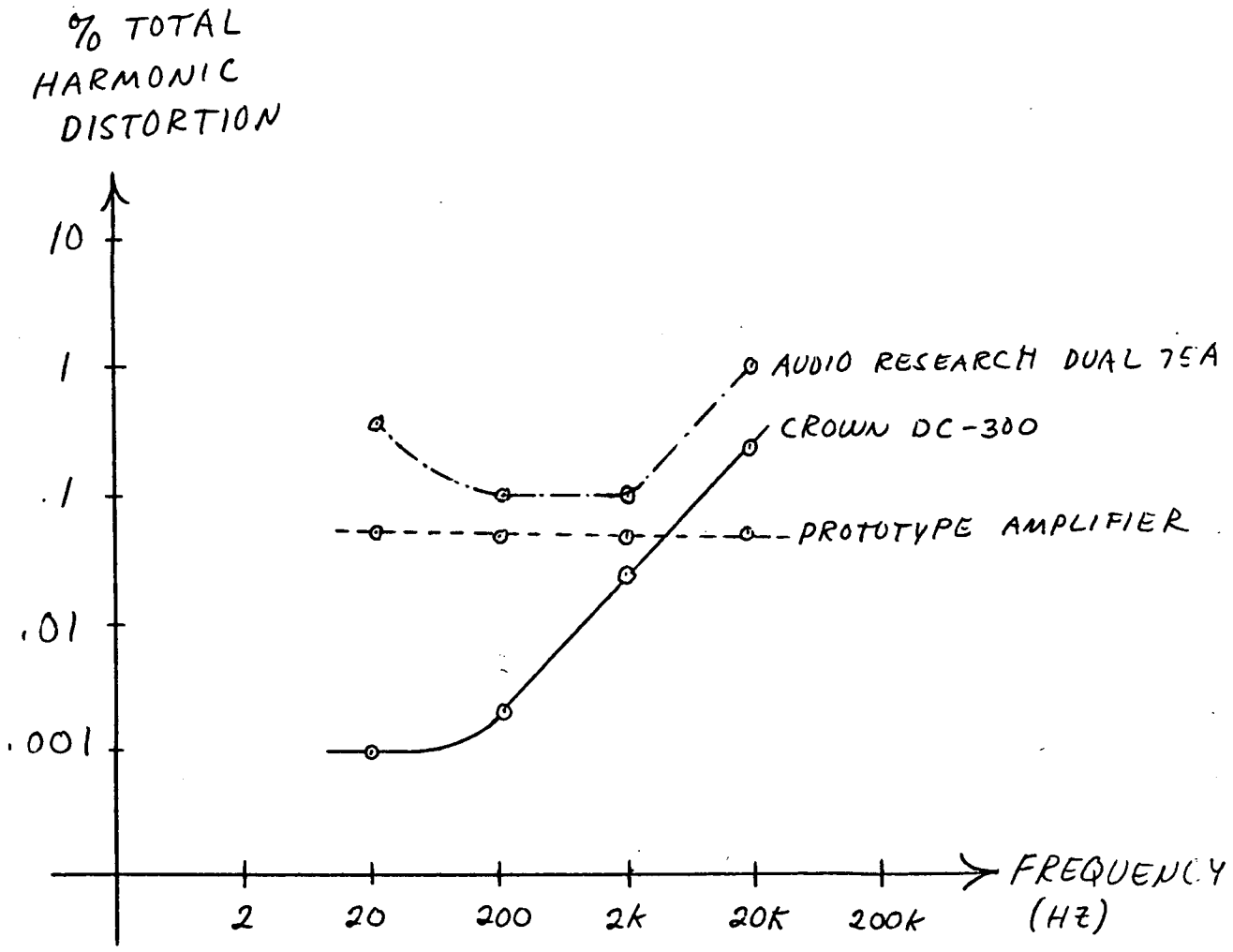

Fig. 12. Harmonic distortion data.

At this point in the project, the measured performance agrees well with that predicted by the theory in Part I.

X. Conclusion

The circuits developed in the project, which realize the constant return difference system presented in Part I, have been described. The specific areas covered were: economics,

non-linear distortion reduction, power supply ripple rejection, thermal stability, realization of the desired transfer functions, power conversion efficiency, and noise reduction. The measured performance of the amplifier indicates that it is superior to presently available high quality commercial power amplifiers.

A subject for future research is the development of output transistor power dissipation limiting circuitry. It is also desirable to design an amplifier with higher output power. This is actually quite simple. An 80 watt rms amplifer can be constructed with no changes in the circuitry other than certain component values. This brings out the universal nature of the design. It is also evident that an isolation network is needed at the output to maintain closed loop stability with highly reactive low impedance loads. These investigations should be completed in the near future.

ACKNOWLEDGEMENT

I wish to thank Profs. Paul F. Duvoisin and James A. Cronvich for their help with the preparation of this paper.

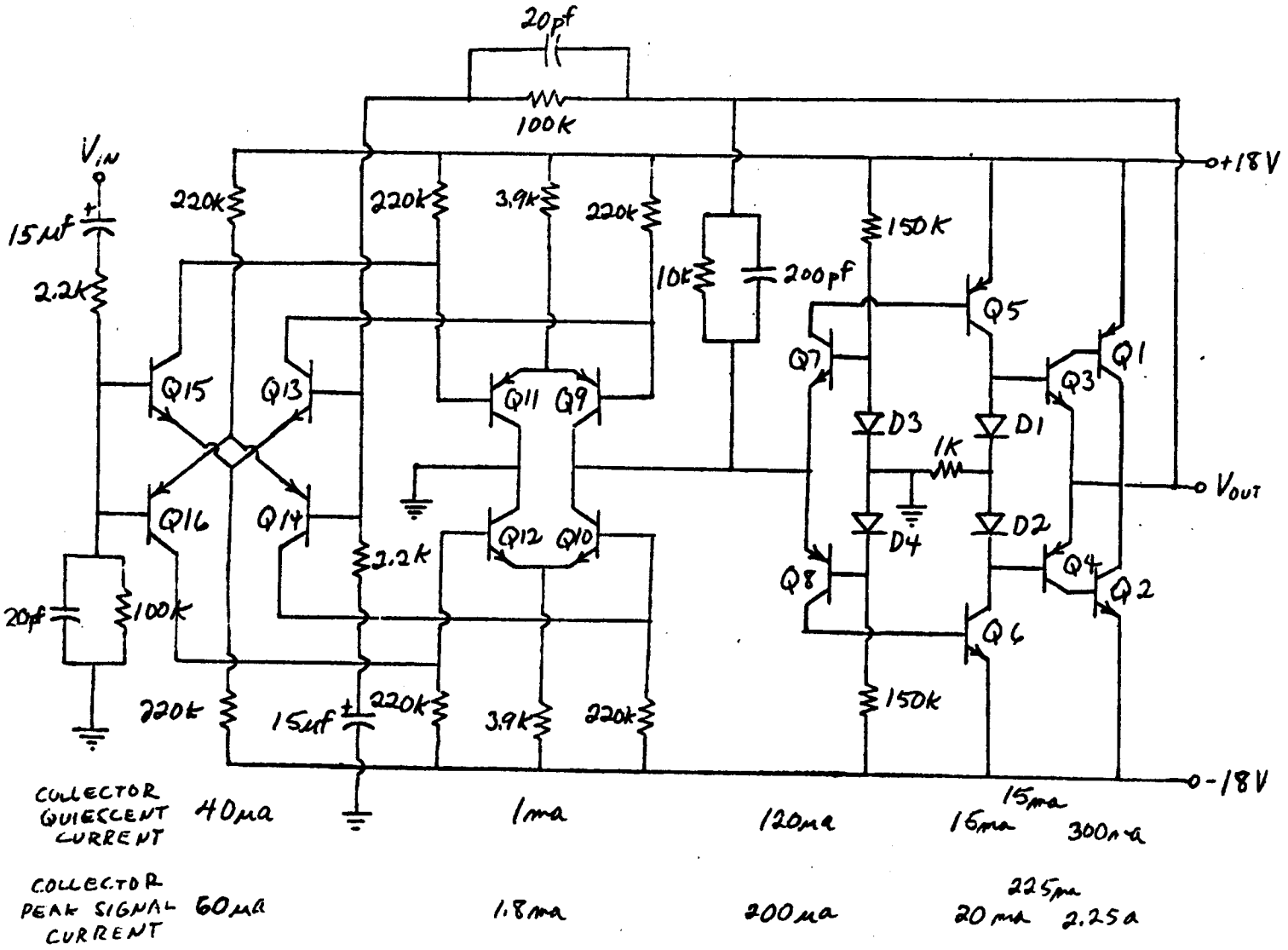

Fig. 13. Schematic diagram of the prototype amplifier.

APPENDIX

CURVE SET NUMBER FOUR
2N4898 Q1

TYPICAL ELECTRICAL CHARACTERISTIC CURVES

AT 25°C AMBIENT TEMPERATURE UNLESS OTHERWISE NOTED

TYPICAL DC CURRENT GAIN VERSUS COLLECTOR CURRENT

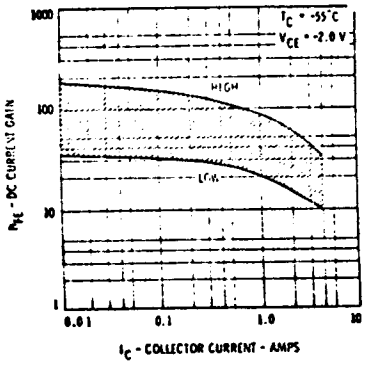

TYPICAL DC CURRENT GAIN VERSUS COLLECTOR CURRENT

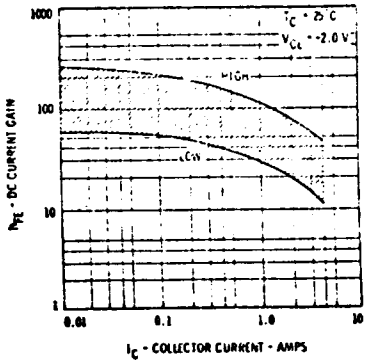

TYPICAL DC CURRENT GAIN VERSUS COLLECTOR CURRENT

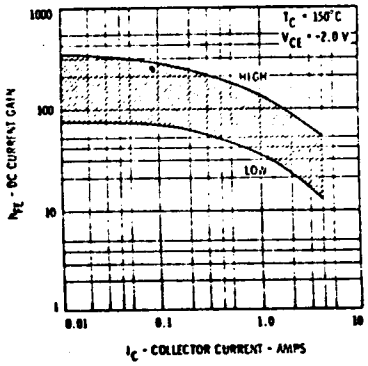

BASE TO EMITTER 'ON' VOLTAGE VERSUS COLLECTOR CURRENT

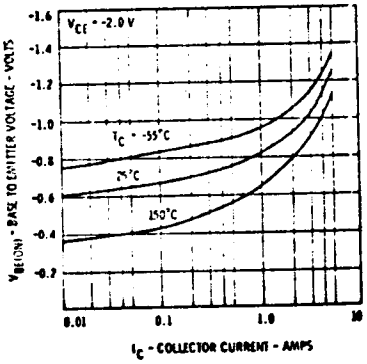

SATURATION VOLTAGES VERSUS COLLECTOR CURRENT

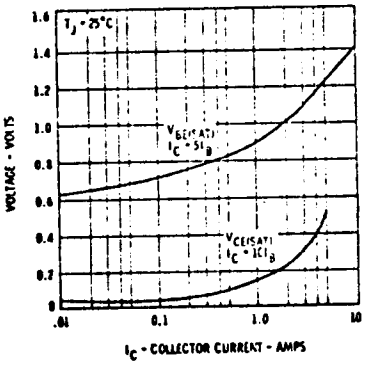

SWITCHING TIMES VERSUS COLLECTOR CURRENT

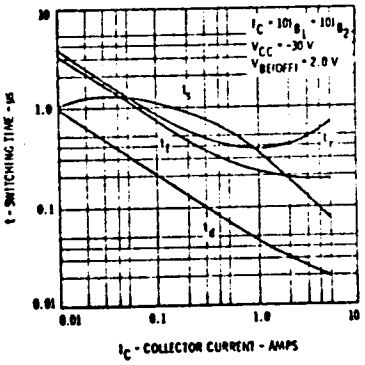

COLLECTOR REVERSE CURRENT VERSUS AMBIENT TEMPERATURE

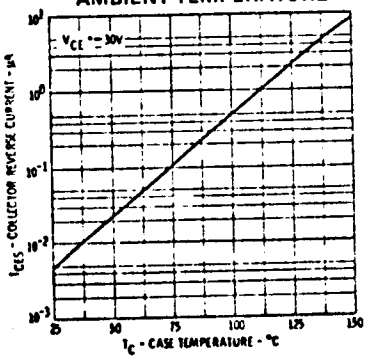

COLLECTOR REVERSE CURRENT VERSUS BASE TO EMITTER VOLTAGE

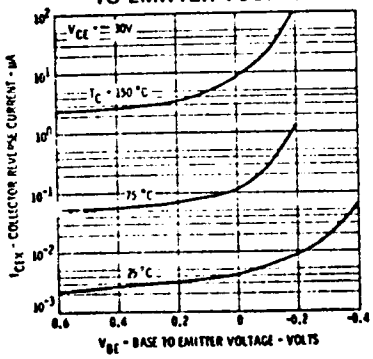

2N4898 Q1

MAXIMUM RATING CURVES

POWER VERSUS TEMPERATURE DERATING CURVE

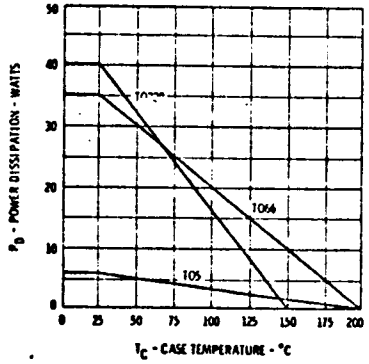

ACTIVE REGION SAFE OPERATING AREA TO5

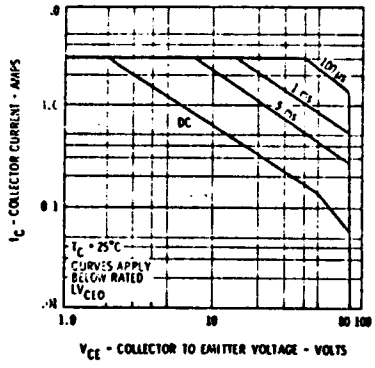

ACTIVE REGION SAFE OPERATING AREA TO66

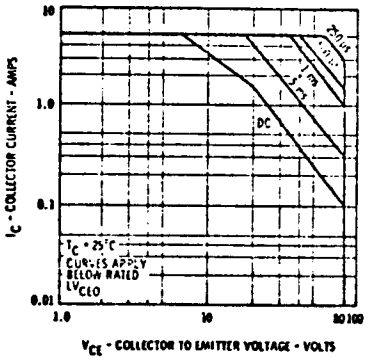

ACTIVE REGION SAFE OPERATING AREA TO220

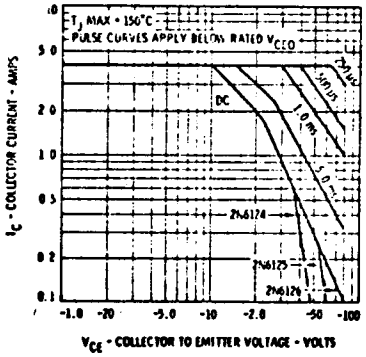

2N4910 Q2

TYPICAL ELECTRICAL CHARACTERISTIC CURVES

AT 25°C AMBIENT TEMPERATURE UNLESS OTHERWISE NOTED

DC CURRENT GAIN VERSUS COLLECTOR CURRENT

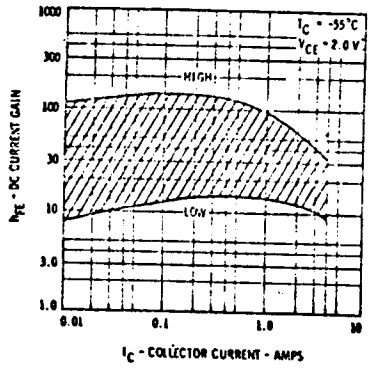

DC CURRENT GAIN VERSUS COLLECTOR CURRENT

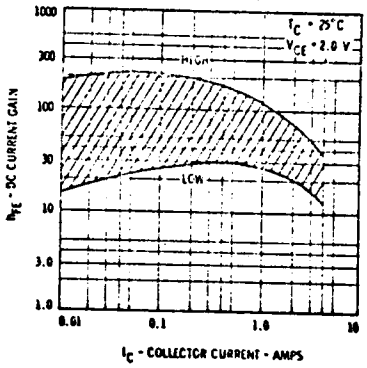

DC CURRENT GAIN VERSUS COLLECTOR CURRENT

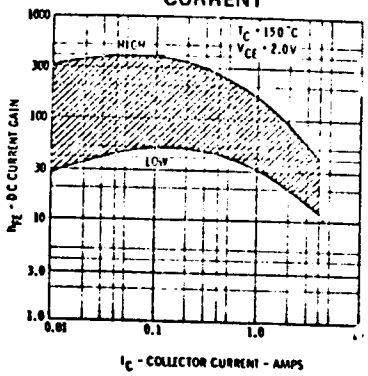

BASE TO EMITTER 'ON' VOLTAGE VERSUS COLLECTOR CURRENT

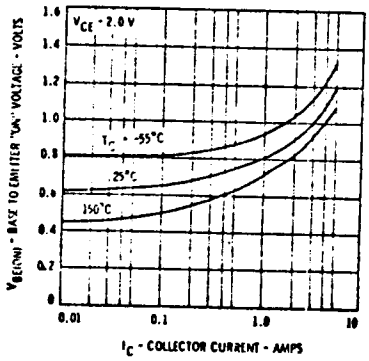

SATURATION VOLTAGES VERSUS COLLECTOR CURRENT

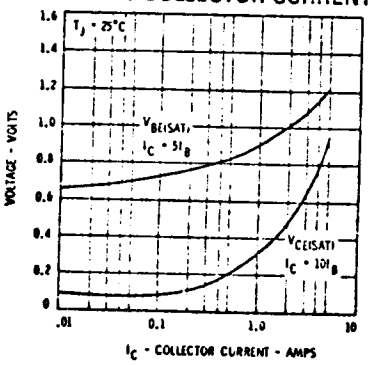

SWITCHING TIMES VERSUS COLLECTOR CURRENT

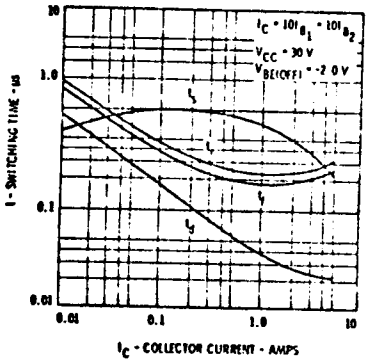

COLLECTOR REVERSE CURRENT VERSUS AMBIENT TEMPERATURE

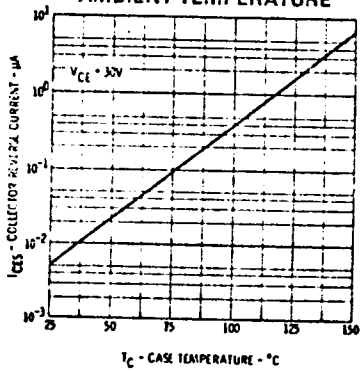

COLLECTOR REVERSE CURRENT VERSUS BASE TO EMITTER VOLTAGE

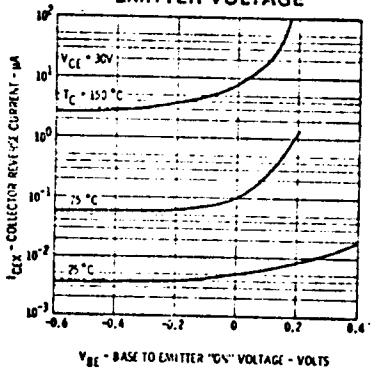

POWER VERSUS TEMPERATURE DERATING CURVE

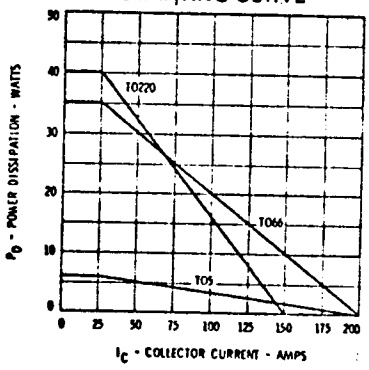

ACTIVE REGION SAFE OPERATING AREA TO5

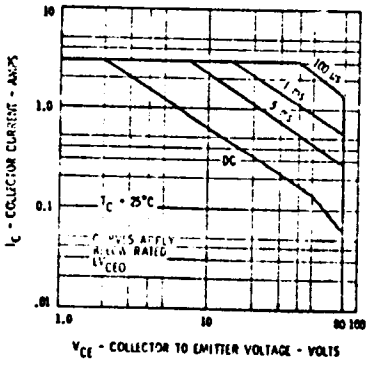

ACTIVE REGION SAFE OPERATING AREA TO66

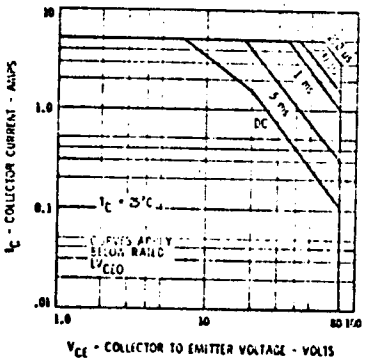

ACTIVE REGION SAFE OPERATING AREA TO220

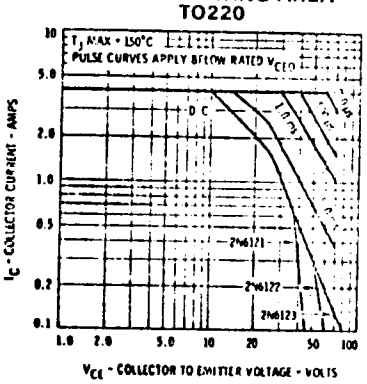

2N2219 Q3, Q4, Q7, Q10, Q12, Q13, Q15

TYPICAL ELECTRICAL CHARACTERISTIC CURVES

AT 25°C AMBIENT TEMPERATURE UNLESS OTHERWISE NOTED

COLLECTOR CHARACTERISTICS

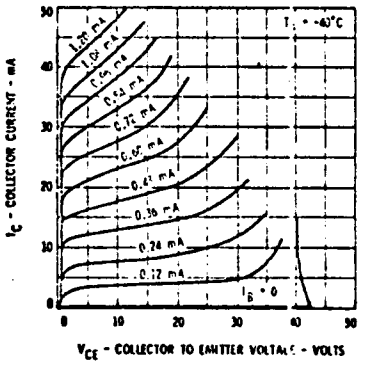

COLLECTOR CHARACTERISTICS

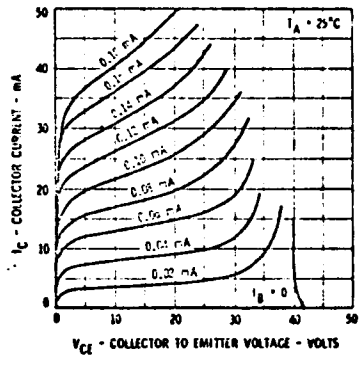

COLLECTOR CHARACTERISTICS

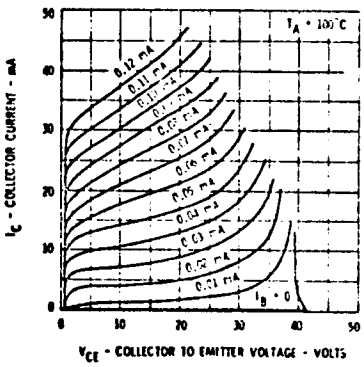

NORMALIZED DC PULSE CURRENT GAIN VERSUS COLLECTOR CURRENT

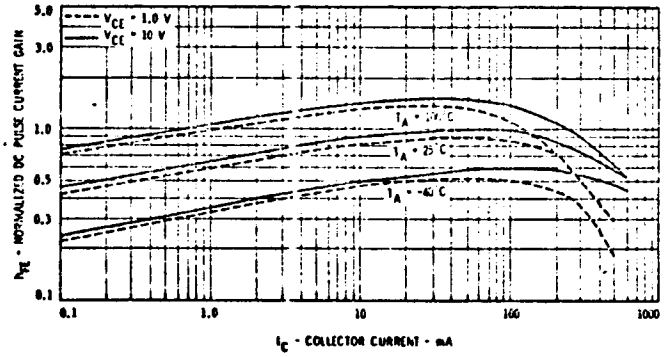

COLLECTOR SATURATION VOLTAGE VERSUS COLLECTOR CURRENT

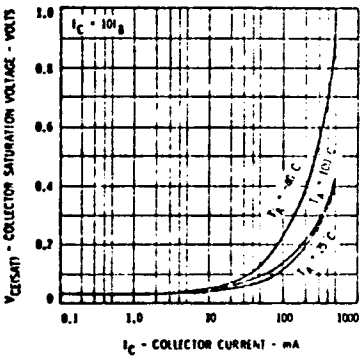

BASE SATURATION VOLTAGE VERSUS COLLECTOR CURRENT

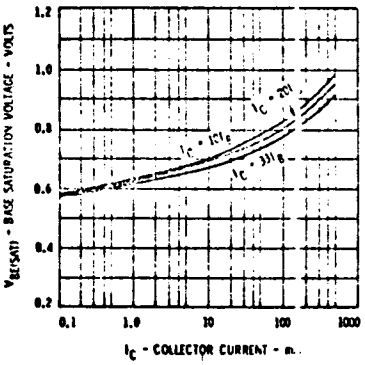

BASE SATURATION VOLTAGE VERSUS AMBIENT TEMPERATURE

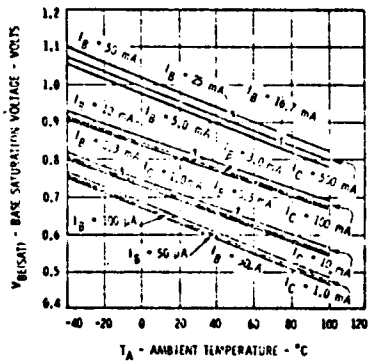

COLLECTOR CUTOFF CURRENT VERSUS AMBIENT TEMPERATURE

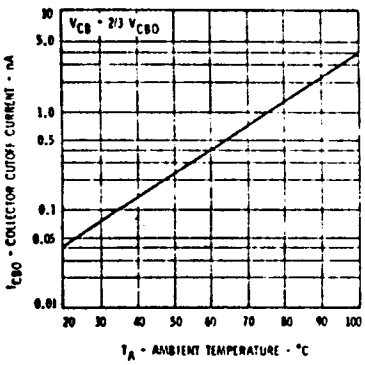

CAPACITANCE VERSUS REVERSE BIAS VOLTAGE

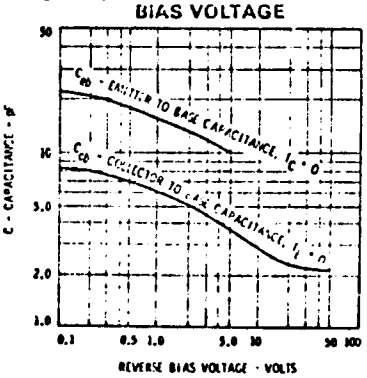

CONTOURS OF CONSTANT GAIN BANDWIDTH PRODUCT

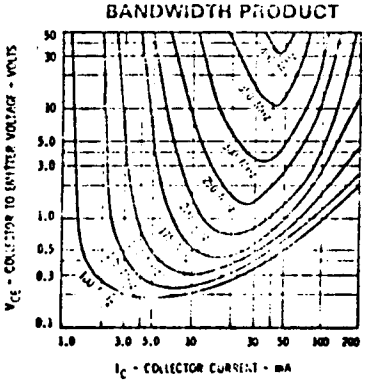

ALLOWABLE POWER DISSIPATION VERSUS AMBIENT TEMPERATURE

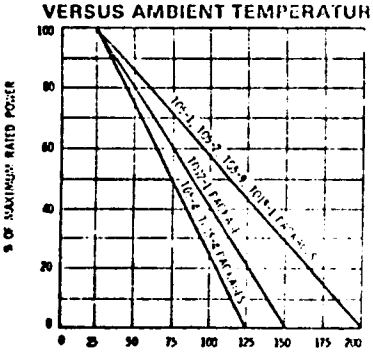

2N2219 Q3, Q4, Q7, Q10, Q12, Q13, Q15

TYPICAL ELECTRICAL CHARACTERISTIC CURVES

AT 25°C AMBIENT TEMPERATURE UNLESS OTHERWISE NOTED

CONTOURS OF CONSTANT NARROW BAND NOISE FIGURE

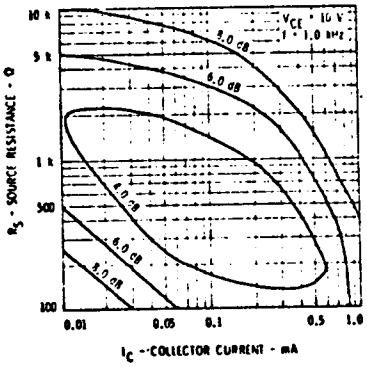

DELAY TIME VERSUS TURN ON BASE CURRENT AND REVERSE BASE EMITTER VOLTAGE

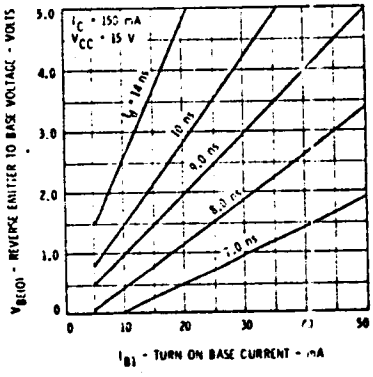

RISE TIME VERSUS COLLECTOR CURRENT AND TURN ON BASE CURRENT

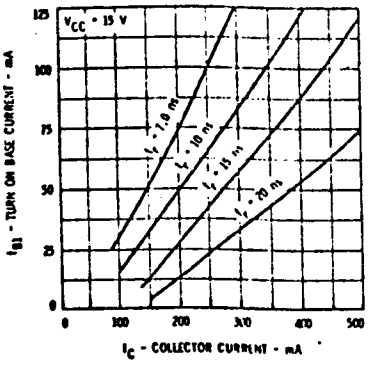

STORAGE TIME VERSUS TURN ON AND TURN OFF BASE CURRENTS

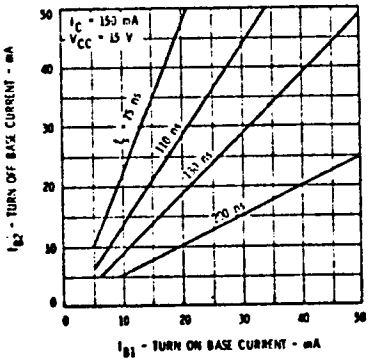

STORAGE TIME VERSUS TURN ON AND TURN OFF BASE CURRENTS

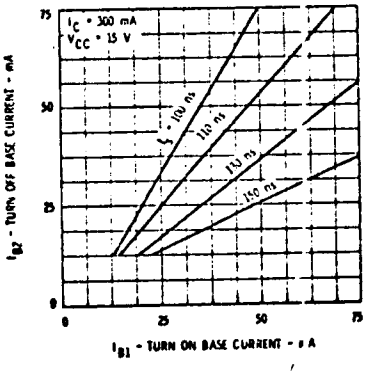

STORAGE TIME VERSUS TURN ON AND TURN OFF BASE CURRENTS

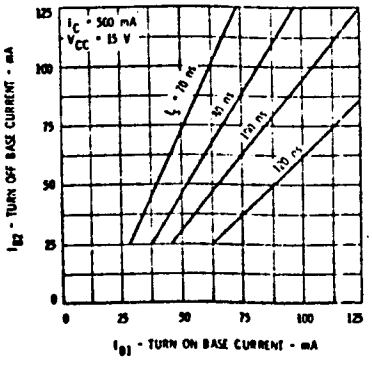

FALL TIME VERSUS TURN ON AND TURN OFF BASE CURRENTS

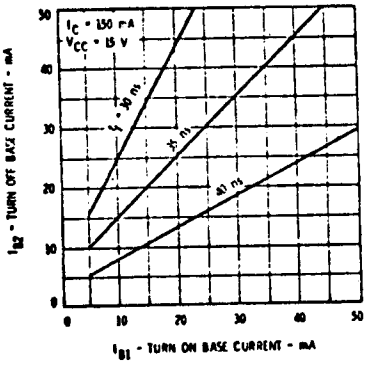

FALL TIME VERSUS TURN ON AND TURN OFF BASE CURRENTS

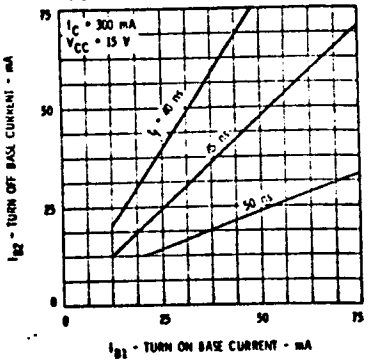

FALL TIME VERSUS TURN ON AND TURN OFF BASE CURRENTS

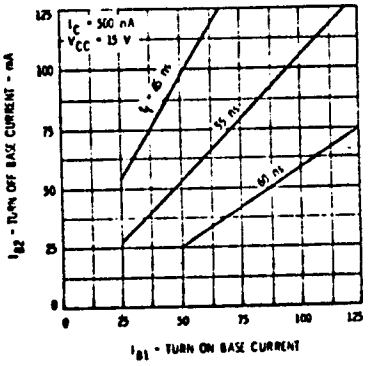

SWITCHING TIME VERSUS COLLECTOR CURRENT

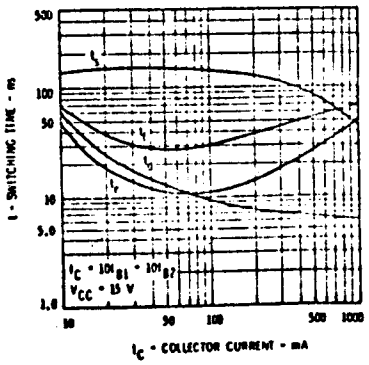

2N2905 Q4, Q5, Q8, Q9, Q11, Q14, Q16

TYPICAL ELECTRICAL CHARACTERISTIC CURVES

AT 25°C AMBIENT TEMPERATURE UNLESS OTHERWISE NOTED

COLLECTOR AND BASE CHARACTERISTICS ACTIVE REGION

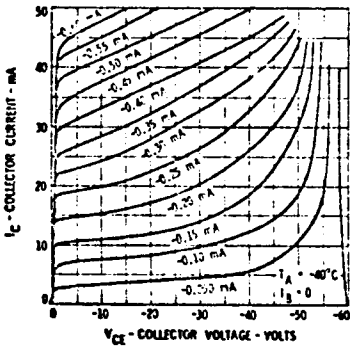

COLLECTOR AND BASE CHARACTERISTICS ACTIVE REGION

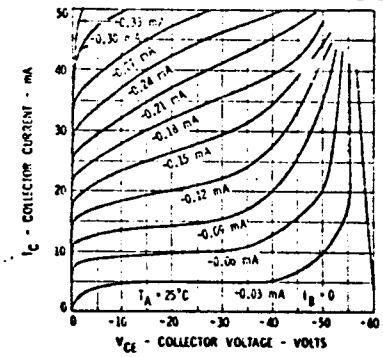

COLLECTOR AND BASE CHARACTERISTICS ACTIVE REGION

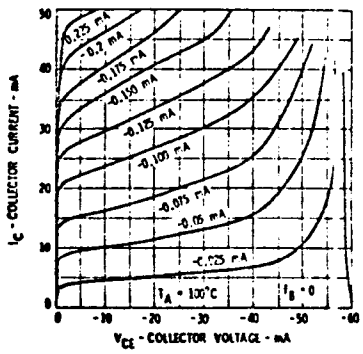

NORMALIZED DC PULSE CURRENT GAIN VERSUS COLLECTOR CURRENT

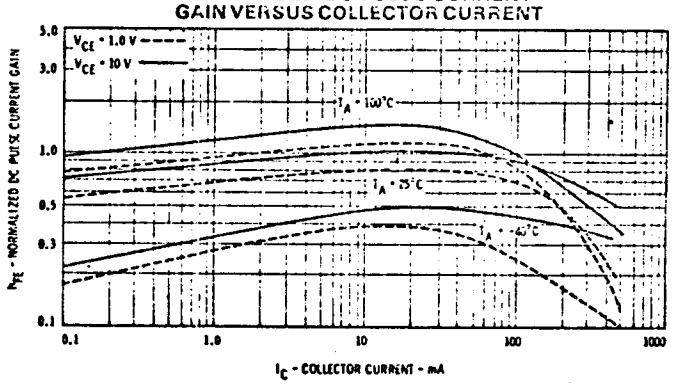

COLLECTOR SATURATION VOLTAGE VERSUS COLLECTOR CURRENT

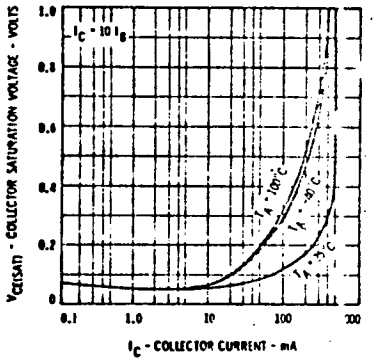

BASE SATURATION VOLTAGE VERSUS COLLECTOR CURRENT

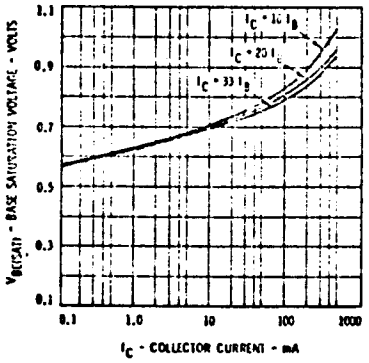

BASE SATURATION VOLTAGE VERSUS AMBIENT TEMPERATURE

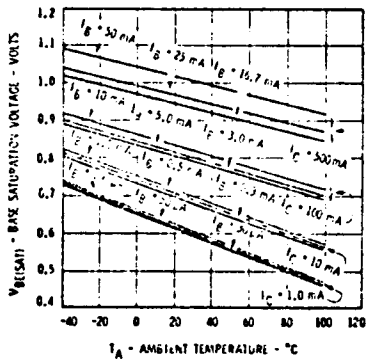

COLLECTOR CUTOFF CURRENT VERSUS AMBIENT TEMPERATURE

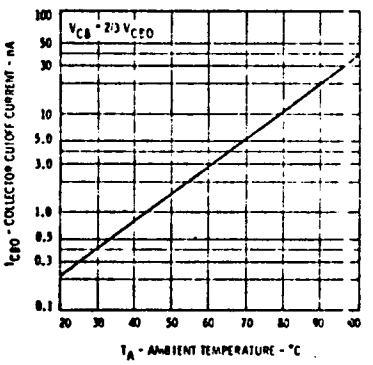

CAPACITANCE VERSUS REVERSE BIAS VOLTAGE

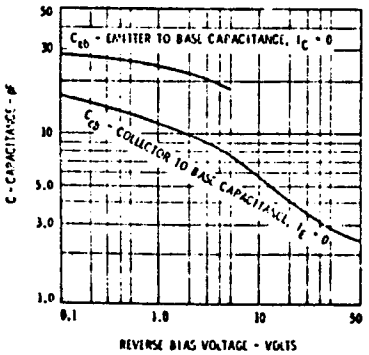

CONTOURS OF CONSTANT GAIN BANDWIDTH PRODUCT

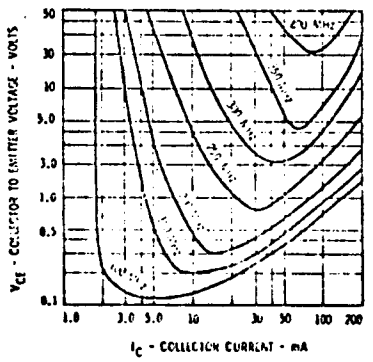

ALLOWABLE POWER DISSIPATION VERSUS AMBIENT TEMPERATURE

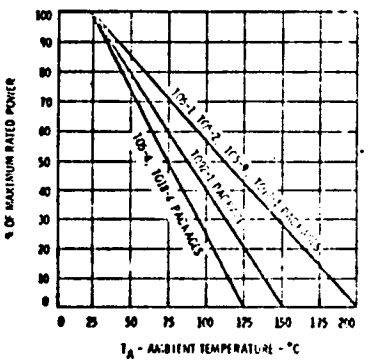

2N2905 Q4, Q5, Q8, Q9, Q11, Q14, Q16

TYPICAL ELECTRICAL CHARACTERISTIC CURVES

AT 25°C AMBIENT TEMPERATURE UNLESS OTHERWISE NOTED

CONTOURS OF CONSTANT NARROW BAND NOISE FIGURE

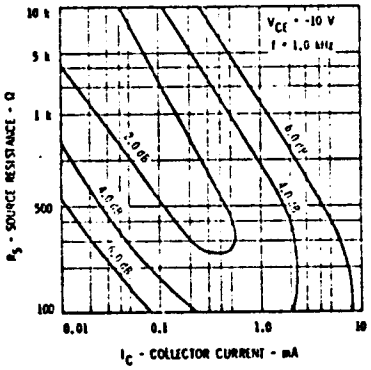

DELAY TIME VERSUS TURN ON BASE CURRENT AND REVERSE BASE TO EMITTER VOLTAGE

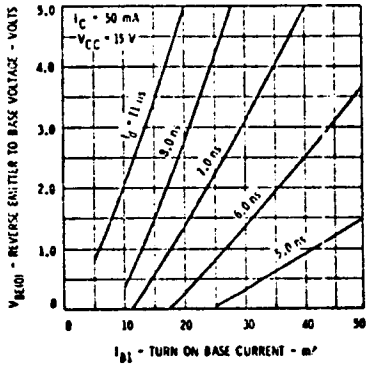

RISE TIME VERSUS COLLECTOR CURRENT AND TURN ON BASE CURRENT

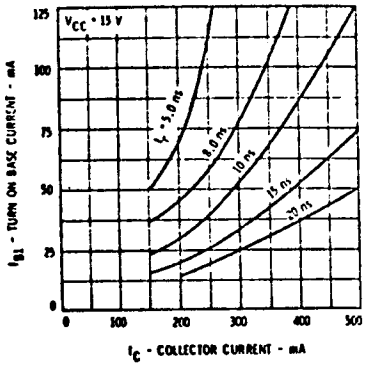

STORAGE TIME VERSUS TURN ON AND TURN OFF BASE CURRENTS

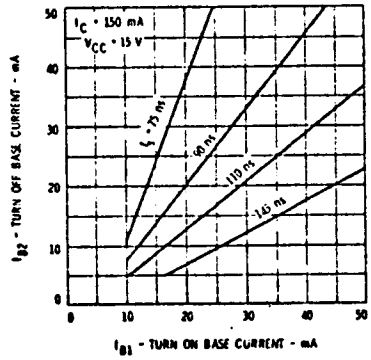

STORAGE TIME VERSUS TURN ON AND TURN OFF BASE CURRENTS

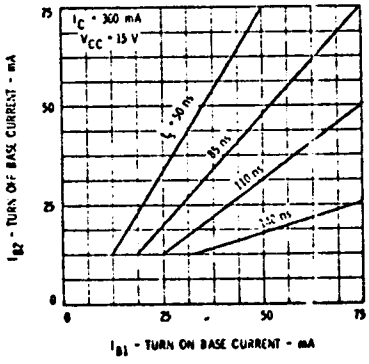

STORAGE TIME VERSUS TURN ON AND TURN OFF BASE CURRENTS

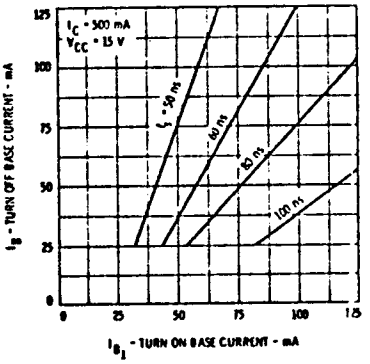

FALL TIME VERSUS TURN ON AND TURN OFF BASE CURRENTS

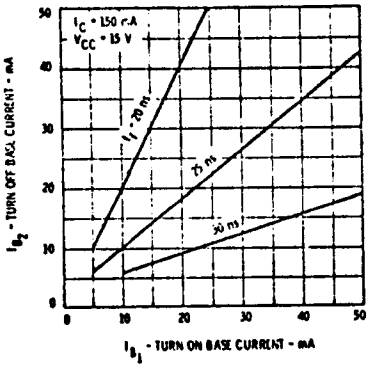

FALL TIME VERSUS TURN ON AND TURN OFF BASE CURRENTS

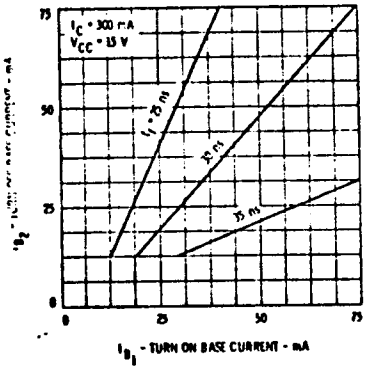

FALL TIME VERSUS TURN ON AND TURN OFF BASE CURRENTS

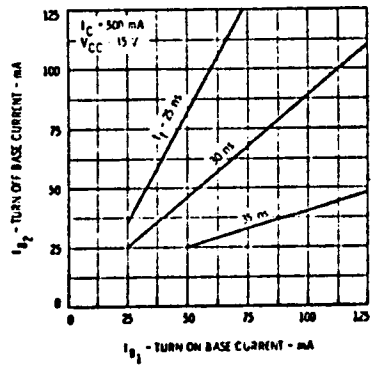

SWITCHING TIME VERSUS COLLECTOR CURRENT

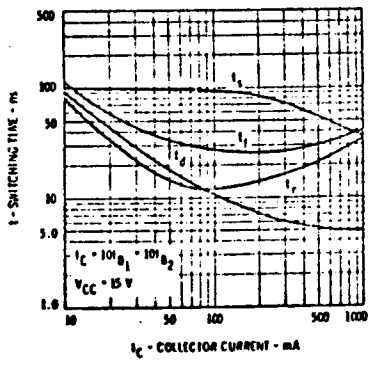

REFERENCES

[1] M. Otala, "Transient distortion in transistorized audio power amplifiers," IEEE Trans. Audio Electroacoust., vol. AU-18, no. 3, Sept. 1970, pp. 234-239.

[2] _____, "Circuit design modifications for minimizing transient intermodulation distortion in audio amplifiers," J. Audio Engr. Soc., vol. 20, no. 5, June 1972, pp. 396-399.

[3] J. Lohstroh, M. Otala, "An audio power amplifier for ultimate quality requirements," IEEE Trans. Audio Electroacoust., vol. AU-21, no. 6, Dec. 1973, pp. 545-550.

[4] J. Melsa, D. Schultz, Linear Control Systems, New York: McGraw-Hill, 1969.

[5] P. Chirlian, Electronic Circuits: Physical Principles, Analysis, and Design, New York: McGraw-Hill, 1971.

[6] Crown DC-300 Owner's Manual.

[7] Audio Research Dual 75A Power Amplifier, Nameplate Data.